LIGAND FIELD PARAMETERS OF SAMARIUM ACTIVATED ALUMINO-BORATE BASED GLASSES **

S. B. Muhammad, I. Abdullahi*, H. I. Muhammad, Y. Usman

Department of Physics Federal University Gusau, Zamfara State Nigeria;
e-mail: sci00316@gmail.com

The nature of the Sm–O bond of samarium-activated alumino-borate-based glasses prepared via the melt-quenching technique was investigated using the Ligand field parameters. Crystal field strength (D_q/B) and Racah parameters B and C were derived from the high-energy region of the absorption spectra. B and C are parameters that describe the influence of the inter-electronic force of repulsion in an atom and hence approximate the strength of the Sm–O bond. The absorption spectra revealed nine bands of transitions from the lower $^6H_{5/2}$ energy level of Samarium to higher $^6P_{3/2}$, $^4I_{11/2}$, ^6H_j, and ^6F_k levels (j = 15/2, 1/2, k = 11/2, 9/2, 7/2, 5/2, and 3/2). The Sm-O bond in the prepared glass samples is less covalent due to the high values of D_q, B, and C. While the crystal field (D_q) and Racah parameters (B and C) decreased with an increase in Sm^{3+} contents, the crystal field strength (D_q/B) increased from 7.87 to 7.89. The observed trend affirmed the attenuation of the ionic nature (increase in the covalency) of the Sm–O bond in the glass host. The observed less covalent nature of Sm–O bond was complemented further by the negative values (–0.7444, –0.9018, –0.8821, and –0.8821 for GS0.5, GS1.0, GS1.5, and GS2.0, respectively) of the evaluated bonding parameters of all the glass samples. The prepared glass samples have the required features for laser applications.

Keywords: *samarium, borate glasses, ligand field, Racah parameters, laser.*

ПАРАМЕТРЫ ЛИГАНДНОГО ПОЛЯ АКТИВИРОВАННЫХ САМАРИЕМ АЛЮМОБОРАТНЫХ СТЕКОЛ

S. B. Muhammad, I. Abdullahi*, H. I. Muhammad, Y. Usman

УДК 621.375.826:546.659

Федеральный университет Гусау, Замфара, Нигерия;
e-mail: sci00316@gmail.com

(Поступила 14 мая 2022)

С использованием параметров поля лиганда исследована природа связи Sm–O в активированных самарием алюмоборатных стеклах, полученных методом закалки расплава. Напряженность кристаллического поля (D_q/B) и параметры Рака B и C получены из высокоэнергетической области спектров поглощения. Параметры B и C описывают влияние межэлектронной силы отталкивания в атоме и, следовательно, аппроксимируют силу связи Sm–O. В спектрах поглощения обнаружены девять полос переходов с нижнего энергетического уровня $^6H_{5/2}$ самария на более высокие уровни $^6P_{3/2}$, $^4I_{11/2}$, ^6H_j и ^6F_k (j = 15/2, 1/2, k = 11/2, 9/2, 7/2, 5/2 и 3/2). Связь Sm–O в образцах стекол менее ковалентна из-за высоких значений D_q, B и C. Кристаллическое поле (D_q) и параметры B и C уменьшаются с ростом содержания Sm^{3+}, D_q/B увеличивается от 7.87 до 7.89. Тенденция подтверждает ослабление ионного характера (увеличение ковалентности) связи Sm–O в стекле-хозяине. Менее ковалентный характер связи Sm–O дополнен отрицательными значениями (–0.7444, –0.9018, –0.8821 и –0.8821 для GS0.5, GS1.0, GS1.5 и GS2.0 соответственно) оцененных параметров склеивания всех образцов стекла. Приготовленные образцы стекла обладают необходимыми характеристиками для лазерных применений.

Ключевые слова: *самарий, боратные стекла, лигандное поле, параметры Рака, лазер.*

** Full text is published in JAS V. 90, No. 5 (http://springer.com/journal/10812) and in electronic version of ZhPS V. 90, No. 5 (http://www.elibrary.ru/title_about.asp?id=7318; sales@elibrary.ru).

Introduction. Rare earth (RE) ions contribute immensely to contemporary scientific and technological advancements, particularly in the field of laser technology [1]. An efficient design of solid-state lasers requires an in-depth understanding of the spectroscopic properties of the RE ion-containing host matrix [2]. These properties are influenced by the nature of the bond formed by the rare earth ion with the host [3]. Consequently, a suitable, reliable, and efficient host is the key issue [4, 5]. Borate-based glasses prove to be stable hosts for rare earth ions due to their uniform and unique spectroscopic attributes [6–9].

The structural and lasing attributes of rare earth-doped glasses are strongly influenced by the nature of the existing RE-O bond [10]. The number of ligand atoms surrounding the RE ion is determined by the RE ion size, whereas the charge determines the strength of the bond formed with the ligand anions [11]. Crystal field strength (D_q/B) and Racah parameters B and C (obtainable from the high energy region of the absorption spectra) are the ligand field parameters used to establish the nature and properties of the RE-O bond and hence unravel the lasing potentials of the concerned host. Crystal field (D_q) arises from the ligand atoms surrounding the rare earth ion, distortion of the 4*f* shell by the ligand field influences the magnetic and spectroscopic properties of the RE ion. D_q is a critical parameter that dictates the probability of numerous laser transitions [12]. For an atom with more than one electron, there exists an inter-electronic force of repulsion between the electrons [13]. Racah parameters B and C are responsive to the local symmetry and hence determine the degree of the inter-electronic force of repulsion and thus the covalency of the RE-O bond. To determine Racah parameters B and C, lower wavelength absorption band positions ν_1, ν_2, and ν_3 are used. The lower the Racah parameters B and C, the higher the covalency of the RE-O bond [14, 15].

The nephelauxetic effect is a shift in the absorption transition energy due to the distortion of 4*f* orbitals caused by the RE complexing ligands [16, 17]. Nehelauxetic ratio (β) and bonding parameter (δ) are also useful in determining the nature of the RE-O bond.

This paper reports the ligand field parameters, nephelauxetic ratio, and bonding parameters of samarium-activated alumino-borate glass prepared using the melt-quenching technique. The aim is to disclose the nature of the Sm–O bond in the proposed glass matrix as a function of Sm^{3+} concentration. This will unravel the potential of the host matrix for laser application. The choice of Sm^{3+} RE and borate-based glass host was influenced by the reports of [18–20].

Experimental. A series of Sm^{3+} activated alumino-borate glasses of composition (70-y)B_2O_3-15$BaSO_4$-15TeO_2-ySm_2O_3 ($0.5 \le y \le 2.0$ mol.%) was prepared using the melt-quenching technique. Analytical grade powder chemicals (Sm_2O_3, B_2O_3, $BaSO_4$, and TeO_2) ≥ 99% purity obtained from Sigma Aldrich were used as constituents. Proper weighing of the chemicals was done using Mettler Toledo digital scale. The chemicals were thoroughly mixed in an alumina crucible and then thawed in an electric furnace at 1300°C for one hour. Quenching of the melt was done on a steel cast preheated at 300°C for 1 h. The glasses were annealed at 400°C for three hours and then allowed to cool to room temperature. Table 1 shows the details of the glass compositions and their codes. The refractive indices of the samples were calculated from the absorption spectra through bandgap energy obtained using Tauc's plot.

TABLE 1. Sample Codes, Compositions and Refractive Indices

Glass code	Starting composition, mol.%	Obtanied Al_2O_3 concentration, mol.%	Refractive index, n
GS0.5	69.5B_2O_3-15$BaSO_4$-15TeO_2-0.5Sm_2O_3	16.0	2.2129
GS1.0	69B_2O_3-15$BaSO_4$-15TeO_2-1Sm_2O_3	17.0	2.2194
GS1.5	68.5B_2O_3-15$BaSO_4$-15TeO_2-1.5Sm_2O_3	17.0	2.2203
GS2.0	68B_2O_3-15$BaSO_4$-15TeO_2-2Sm_2O_3	18.0	2.2288

Room temperature UV-Vis-NIR absorption analysis was carried out at a range of 300 to 1800 nm using a 3600Plus Shimadzu spectrometer. Emission spectra under 402 nm excitation and through a wavelength range of 300 to 750 nm were recorded using a Fluoromax-4C spectrofluorometer. XRD analysis of the powdered glasses was done using a Rigakusmartlab diffractometer through 2θ range of 0 to 100°. The elemental composition was analyzed using energy dispersive X-ray measurements in the range of 0 to 20 keV at a resolution of 10^{-6} m, using an Oxford X-Max^{N}100TLE fluorescence spectrometer. The densities of the glass samples were calculated using Archimedes's principle.

Results and discussion. *XRD and EDX analyses.* The absence of sharp peaks from the X-ray diffraction (XRD) pattern of the synthesized glasses confirmed their amorphous nature [21]. Figure 1 elucidates the XRD pattern of the as-quenched samples. Figure 2 illustrates the EDX spectra of all the developed glasses in the energy range of 0–20 keV. The successful incorporation of the individual elements in the glass sample and their corresponding wt.% is evident therein. Aluminium was manifested from the employed alumina crucible. Moreover, the uniformity and homogeneity of the individual elements as revealed by EDX-mapping analysis are shown in Fig. 3.

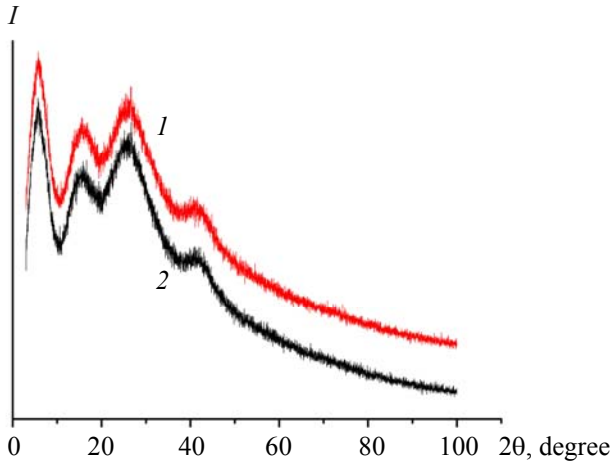

Fig. 1. XRD pattern of the synthesized glasses: CS0.5 (*1*), and CS1.0 (*2*).

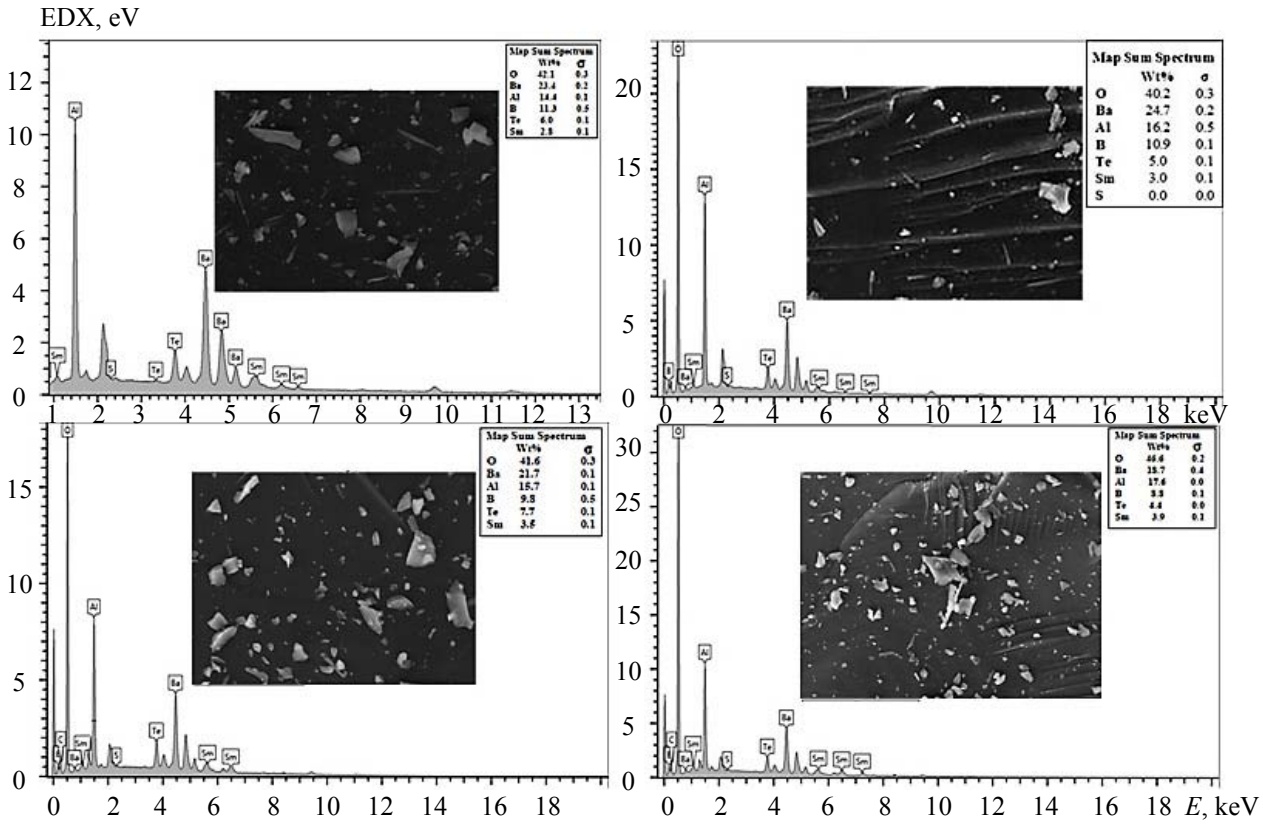

Fig. 2. EDX quant results of the synthesized glasses along with the electron layered image.

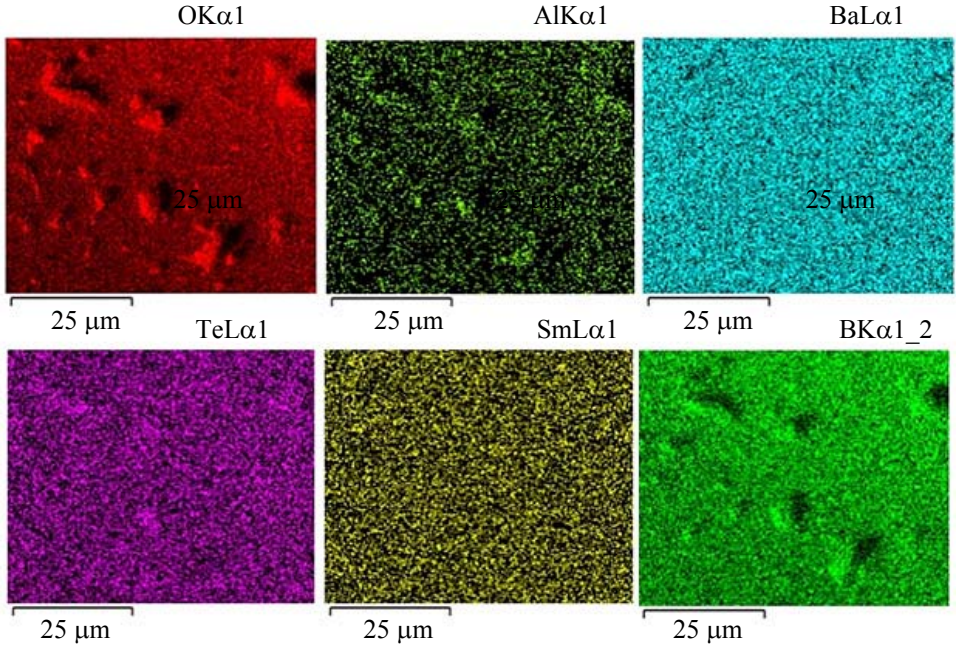

Fig. 3. EDX elemental mapping of the glasses showing the elemental homogeneous distribution.

Optical absorption. UV-Vis-NIR absorption spectroscopy is among the most important optical analytical techniques because of its simplicity, high precision, flexibility, less time consumption, and cost-effectiveness [22]. It involves the study of electronic transitions from lower to higher energy levels due to the absorption of electromagnetic radiation in the UV-Vis region by a given sample. Electronic energy levels are largely spaced when compared with vibrational or rotational energy levels; as such, only photons with sufficient energy can cause electronic transitions. Figure 4 depicts the high and low energy region absorption spectra of the synthesized glasses. While the low energy region discloses three eminent transitions of ${}^6H_{5/2}\rightarrow{}^6P$, ${}^6H_{5/2}\rightarrow{}^4G$, and ${}^6H_{5/2}\rightarrow{}^4I$ terms, the high energy region displays seven distinct transitions of ${}^6H_{5/2}\rightarrow{}^6F$ and ${}^6H_{5/2}\rightarrow{}^6H$ terms. Generally, the absorption spectra revealed nine prominent ${}^6H_{5/2}\rightarrow{}^6P_{3/2}$, ${}^6H_{5/2}\rightarrow{}^4I_{11/2}$, ${}^6H_{5/2}\rightarrow{}^6H_j$, and ${}^6H_{5/2}\rightarrow{}^6F_k$ (j = 15/2, 1/2, k = 11/2, 9/2, 7/2, 5/2, and 3/2, respectively) bands of samarium transitions [23–25]. It is known that Sm^{3+} ions do not absorb from the ground state in the 570–900 nm region; hence, the absence of absorption peaks in the region, which may be attributed to forbidden spin-selection rules [26, 27]. Hyper-sensitive transitions ${}^6H_{5/2}\rightarrow{}^6F_{3/2}$, ${}^6H_{5/2}\rightarrow{}^6F_{5/2}$, ${}^6H_{5/2}\rightarrow{}^6F_{7/2}$, and ${}^6H_{5/2}\rightarrow{}^6F_{9/2}$ adhered to the quadropole selection rules $|\Delta J| \leq 2$, $|\Delta L| \leq 2$ and $\Delta S = 0$ [28]. Optical properties and ligand field parameters (D_q, B, and C) of the prepared samples are derivatives of the lower wavelength region of the measured absorption spectra. The optical and physical properties of the prepared glass systems as deduced from our earlier report [27] are presented in Table 2.

TABLE 2. Physical and Optical Properties of the Synthesized Glasses

Parameter	Glass sample			
	GS0.5	GS1.0	GS1.5	GS2.0
Indirect bandgap, eV	2.511	1.826	2.169	2.655
Direct bandgap, eV	3.612	3.458	3.533	3.582
Urbach energy, eV	0.535	0.560	1.834	1.790
Dielectric constant	3.091	3.095	3.098	3.104
Optical dielectric constant	2.091	2.095	2.098	2.104
Reflection loss, %	7.556	7.572	7.585	7.608
Electronic polarizability	21.166	21.189	20.753	20.667
Molar mass, g/mol	109.073	110.468	111.864	113.259
Molar volume, cm^3/mol	39.766	38.913	38.691	38.634
Polaron radius, 10^{-10} m	2.052	1.617	1.410	1.280
Inter-ionic distance, 10^{-10} m	5.093	4.013	3.499	3.177

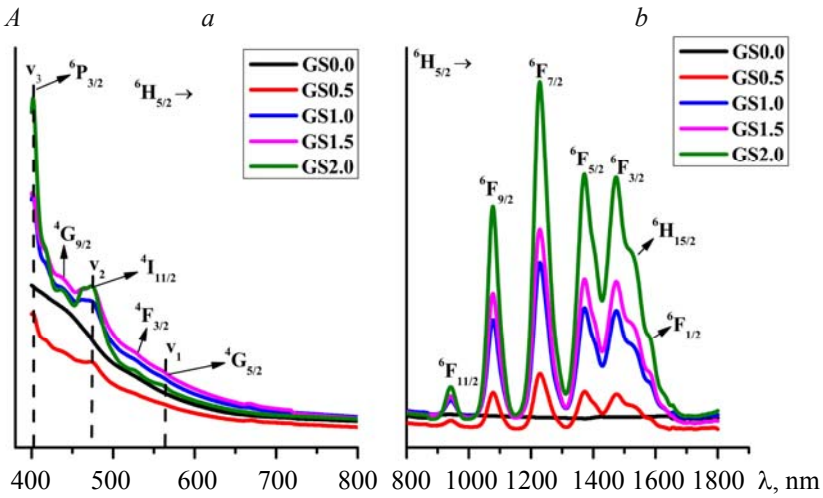

Fig. 4. (a) Lower wavelength absorption region, (b) Higher wavelength absorption region for the synthesized glasses.

Ligand field parameters. Racah parameters (B and C). Using the measured absorption spectra, the covalency of the Sm–O bond in the prepared glass matrices was explored via Racah parameters. For the evaluation of B and C, the absorption bands ν_1, ν_2, and ν_3 are selected from the high energy region where the transitions are allowed, as shown in Fig. 4, wherein Eqs. (1) to (4) [14, 29] were used in the evaluation process:

$$D_q = \nu_1 / 10 , \tag{1}$$

$$B = \frac{2\nu_1^2 + \nu_2^2 - 3\nu_1\nu_2}{15\nu_2 - 27\nu_1} , \tag{2}$$

$$C = \left(\nu_3 - 4B - 10D_q\right) / 3 . \tag{3}$$

Table 3 presents the values of the calculated ligand field parameters. The magnitude of B decreased with an increase in Sm^{3+} contents from 316.72 cm^{-1} for GS0.5 to 315.86 cm^{-1} for GS2.0, while in a similar trend, the value of C decreased from 4348 cm^{-1} for GS0.5 to 4346.2 cm^{-1} for GS2.0. The decay in the values of B and C with an increase in Sm^{3+} concentration indicated the growth in the covalency of the Sm–O bond [30]. The symmetry of local Sm^{3+} sites decreased with Sm^{3+} contents due to the delocalization of additional 4*f* electrons [14, 29]. The observed B and C trends are required for laser applications [29].

TABLE 3. Ligand Field Parameters for the Prepared Glass Samples

Glass code	Ligand field parameters				
	B (±0.01 cm^{-1})	C (±0.06 cm^{-1})	D_q (±0.004 cm^{-1})	D_q/B	Reference
GS0.5	316.72	4348.00	2493.80	7.87	This study
GS1.0	316.41	4346.79	2493.50	7.88	This study
GS1.5	315.94	4345.42	2493.00	7.89	This study
GS2.0	315.86	4346.2	2492.90	7.89	This study
TZS1	244.68	1886.29	1834.86	7.50	[14]
MZSPEAg0.1	82.85	8274.94	2544.53	30.71	[28]
NiO0.05	1018.90	3601.80	870.00	–3.45	[30]
CsPF6:Mn^{4+}	617.00	3787.00	2127.00		[31]

Crystal field variables (D_q and D_q/B). The evaluated crystal fields (D_q) and crystal field strength (D_q/B) were outlined in Table 3. The observed higher value of the crystal field strength (>2.3) for all the glasses suggests the concentration of Sm^{3+} ions in a strong crystal field environment within the glass host [32, 33]. The increase in the values of the crystal field strength with an increase in Sm^{3+} contents accelerates the switching of the ligand field from strong to stronger ligand sites [34, 35]. Hence the strength of the Sm–O

bond, and by extension, the optical properties of the present host, are tunable by varying the Sm^{3+} concentration. Figure 5 exhibits the variation of D_q/B as a function of Sm^{3+} contents. The observed strong ligand field strength environment of the studied host is an indication of its ability to strongly resist wear and thermal shock; a required feature for laser application [36].

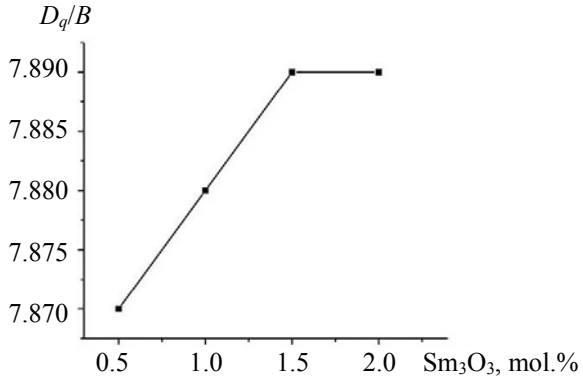

Fig. 5. Variation of crystal field strength as a function of Sm^{3+} content.

Nephelauxetic ratio and bonding parameter. It was observed that when rare earth ions are doped in glass matrices, the center peaks of the absorption transitions are slightly displaced in comparison with that in an aqueous solution. This effect is known as the Nephelauxetic effect and is a consequence in response to the deformation of 4*f* orbitals. The nephelauxetic ratios (β) for all the absorption transitions herein were obtained by comparing the wavelength with that in an aqueous solution. Being sensitive to the Sm^{3+} environment, β can be used in unraveling the nature of Sm^{3+}-O bonding through σ. From the β values, σ for each sample was determined by applying the equations of [27]. The evaluated bonding parameters of the synthesized glasses are –0.7444, –0.9018, –0.8821, and –0.8821 for samples GS0.5, GS1.0, GS1.5, and GS2.0, respectively. These values confirmed the migration of the Sm–O bond from ionic to covalent nature with an increase in Sm^{3+} content.

Conclusions. The evaluated ligand field parameters D_q, B, and C of the prepared glasses ascertained the nature of Sm–O bonding and hence disclosed the spectroscopic attributes of the glass hosts. Reduction in the values of B and C with increasing Sm^{3+} contents signified the delocalization of 4*f* electrons and the subsequent increase in the covalency of the Sm–O bond. The high value of D_q/B (7.87 to 7.89 for GS0.5 to GS2.0) is a testimony to the strength of the glasses. Generally, the synthesized glasses are less covalent as confirmed by the negative values of the bonding parameter but the covalency increases with increasing Sm^{3+} contents. The prepared glass samples have the required features for solid-state laser applications.

This work was supported by the Nigeria Tertiary institutions trust fund (Tetfund) under the Institutional based research Grant with the following subheading TETF/DR&D/CE/UNIV/ GUSAU/IBR/2020/VOL.1.

REFERENCES

1. S. Balaji, P. A. Azeem, R. R. Reddy, *Phys. B*, **394**, 62–68 (2007).
2. A. I. Yenzhyieuski, M. V. Bogdanovich, G. I. Ryabtsev, V. V. Suprun, A. V. Grigor'ev, A. G. Ryabtsev, M. A. Shchemelev, *J. Appl. Spectrosc.*, **76**, 505–510 (2009).
3. J. H. Choi, *J. Appl. Spectr.*, **82**, 360–366 (2015).
4. G. Lakshminarayana, M. K. Kawa, S. O. Baki, A. Lira, U. Caldino, I. V. Kityk, *Opt. Mater.* (*Amst.*), **72**, 380–391 (2017).
5. I. I. Kindrat, B. V. Padlyak, R. Lisiecki, *Opt. Mater.* (*Amst.*), **49**, 241–248 (2015).
6. V. Uma, M. Vijayakumar, K. Marimuthu, G. Muralidharan, *J. Mol. Struct.*, **1151**, 266–276 (2018).
7. P. Van Do, V. Phi, V. Xuan, L. Xuan, L. Duy, T. Ngoc, *Opt. Mater.* (*Amst.*), **55**, 62–67 (2016).
8. K. Annapoorani, K. Maheshvaran, S. Arunkumar, N. S. Murthy, K. Marimuthu, *Spectrochim. Acta A: Mol. Biomol. Spectrosc.*, **135**, 1090–1098 (2014).
9. K. Annapoorani, N. S. Murthy, T. R. Ravindran, K. Marimuthu, *J. Lumin.*, **171**, 19–26 (2016).
10. P. J. van Der Put, *The Inorganic Chemistry of Materials*, Springer, New York (1998).

11. K. Bhargavi, M. S. Reddy, P. R. Rao, N. N. Rao, M. S. Rao, V. R. Kumar, N. Veeraiah, *Mater. Res. Bull.*, **47**, 267–273 (2012).
12. B. M. Walsh, *Judd-Ofelt Theory: Principles and Practices*, Springer, The Netherlands (2006).
13. A. Bartecki, K. Kurzak, *Pol. Des Sci.*, **29**, 299–305 (1982).
14. Y. A. Tanko, S. K. Ghoshal, M. R. Sahar, *J. Mol. Struct.*, **1117**, 64–68 (2016).
15. A. M. Hamza, M. K. Halimah, F. D. Muhammad, K. T. Chan, *J. Lumin.*, **207**, 497–506 (2019).
16. V. S. Sastri, J.-C. G. Bunzli, V. R. Rao, G. V. S. Rayudu, J. R. Perumareddi, *Modern Aspects of Rare Earths and their Complexes*, Elsevier B. V., Amsterdam (2003).
17. Z. G. Mazurak, M. Czaja, *Opt. Mater.* (*Amst.*), **33**, 506–510 (2011).
18. G. E. Malashkevich, V. N. Sigaev, N. V. Golubev, E. K. Mamadzhanova, A. A. Sukhodola, A. Paleari, P. D. Sarkisov, A. N. Shimko, *Mater. Chem. Phys.,***137**, 48–54 (2012).
19. G. E. Malashkevich, A. N. Shimko, A. P. Stupak, I. V. Prusova, K. N. Nischev, V. M. Kyashkin, A. A. Kornienko, E. B. Dunina, A. V. Semchenko, I.I. Sergeev, *J. Appl. Spectrosc.*, **86**, 584–589 (2019).
20. M. A. Marzouk, S. M. Abo-Naf, H. A. Zayed, N. S. Hassan, *J. Appl. Spectrosc.*, **84**, 162–169 (2017).
21. I. Hossain, N. K. Shekaili, H. Wagiran, *J. Appl. Spectrosc.*, **82**, 149–152 (2015).
22. K. H. S. Shaaban, A. A. El-maaref, M. Abdelawwad, Y. B. Saddeek, H. Wilke, H. Hillmer, *J. Lumin.*, **196**, 477–484 (2018).
23. W. T. Carnall, P. R. Fields, K. Rajnak, *J. Chem. Phys.*, **49**, 4424–4442 (1968).
24. S. Jain, R. Singh, *J. Chem. Pharm. Res.*, **3**, 1–5 (2011).
25. P. Srivastava, *J. Appl. Spectrosc.*, **84**, 521–528 (2017).
26. S. Sailaja, C. Nageswara Raju, C. Adinarayana Reddy, B. Deva Prasad Raju, Y. D. Jho, B. Sudhakar Reddy, *J. Mol. Struct.*, **1038**, 29–34 (2013).
27. I. Abdullahi, S. Hashim, S.K. Ghoshal, *J. Lumin.*, **216**, 116686 (2019).
28. F. Nawaz, M. R. Sahar, S. K. Ghoshal, A. Awang, R. J. Amjad, *J. Lumin.*, **2014**, 90–96 (2014).
29. I. Mohammed, S. K. Ghoshal, R. Ari, S. Aishah, *J. Lumin.*, **216**, 116713 (2019).
30. S. S. Sastry, B. R. V. Rao, T. Vishwam, *Indian J. Phys.*, **89**, 73–80 (2014).
31. A. M. S. Farouk, Y. M. Abo-Zeid, M. A. Khaled, I. Kashif, *J. Mater. Sci. Mater. Electron.*, **6**, 393–396 (1995).
32. Y. Chen, Z. Yang, Q. Wang, M. Rong, Q. Zhou, Z. Wang, *Dalt. Trans.*, **48**, 10901–10906 (2019).
33. Y. Liu, T. Wang, X. Zhang, C. Cao, L. Yang, Y. Huang, S. Liao, *J. Mater. Sci. Mater. Electron.*, **30**, 1870–1877 (2019).
34. M. A. Hassan, F. M. Ebrahim, M. G. Moustafa, Z. M. A. El-fattah, M. M. El-okr, *J. Non. Cryst. Solids*, **515**, 157–164 (2019).
35. I. Abdullahi, S. Hashim, S. K. Ghoshal, A. U. Ahmad, *Mater. Chem. Phys.*, **247**, 122862 (2020).
36. W. F. James, *Handbook of Optical Materials*, CRC Press, New York (2003).